Journal of
Composites Science

MDPI

Article

Comparison of Bending Properties of Sandwich Structures Using Conventional and 3D-Printed Core with Flax Fiber Reinforcement

Viktor Brejcha [1], Martin Böhm [1], Tomáš Holeček [2], Miloš Jerman [1], Klára Kobetičová [1], Ivana Burianová [1], Robert Černý [1] and Zbyšek Pavlík [1,*]

[1] Department of Material Engineering and Chemistry, Faculty of Civil Engineering, Czech Technical University in Prague, 166 29 Prague, Czech Republic; viktor.brejcha@fsv.cvut.cz (V.B.); martin.bohm@fsv.cvut.cz (M.B.); milos.jerman@fsv.cvut.cz (M.J.); klara.kobeticova@fsv.cvut.cz (K.K.); burianova.i@icloud.com (I.B.); cernyr@fsv.cvut.cz (R.Č.)
[2] Faculty of Forestry and Wood Sciences, Czech University of Life Sciences Prague, 165 00 Prague, Czech Republic; holecekt@fld.czu.cz
* Correspondence: pavlikz@fsv.cvut.cz

Abstract: The growing demand for sustainable composites has increased interest in natural fiber reinforcements as alternatives to synthetic materials. This study evaluates the bending properties of sandwich structures with flax fibers and 3D-printed lightweight foaming PLA cores compared to conventional designs using glass fibers and traditional cores. Three-point bending tests (EN 310) and density profile analysis showed that, despite its lower density, the 3D-printed foaming PLA core achieved a modulus of elasticity of 2269.19 MPa and a bending strength of 31.46 MPa, demonstrating its potential for lightweight applications. However, natural fibers influenced resin absorption, affecting core saturation compared to glass fibers. The use of bio-based epoxy and foaming PLA contributes to a lower environmental footprint, while 3D printing enables precise material optimization. These findings confirm that 3D-printed cores offer a competitive and sustainable alternative, with future research focusing on further optimization of internal structure to enhance mechanical performance.

Keywords: foam core; 3D-printed core; balsa wood; glass fiber; flax fiber; density profile; bending strength; sustainable composite

Academic Editor: Francesco Tornabene

Received: 27 January 2025
Revised: 7 April 2025
Accepted: 8 April 2025
Published: 9 April 2025

Citation: Brejcha, V.; Böhm, M.; Holeček, T.; Jerman, M.; Kobetičová, K.; Burianová, I.; Černý, R.; Pavlík, Z. Comparison of Bending Properties of Sandwich Structures Using Conventional and 3D-Printed Core with Flax Fiber Reinforcement. *J. Compos. Sci.* **2025**, *9*, 182. https://doi.org/10.3390/jcs9040182

1. Introduction

Technological advancements and growing sustainability demands are reshaping composite use in engineering and construction. Over the past decade, lightweight carbon fiber composites have dominated, but the focus is now shifting toward recyclable and bio-based composites [1]. In 2023, the global composite materials market was valued at USD 41 billion, with assemblies using composite parts adding USD 105 billion. Between 2010 and 2023, the sector demonstrated a compound annual growth rate (CAGR) of 2–4% [2]. Future growth is expected to accelerate to 8.2% annually between 2022 and 2030 [3], driven by increased demand for recyclable composites and bio-based alternatives to traditional materials [4,5].

Glass fiber maintained its dominant position in global fiber production in 2023, accounting for 77% of total output, followed by carbon fiber at 18%, with natural fibers contributing only 4% [6]. Total fiber production increased from 12 million tons in 2021 to 13 million tons by 2023 [7]. Composite materials find extensive application across multiple sectors, including aerospace, energy, transportation, and construction. Among these, the aerospace sector is projected to experience the highest CAGR (7%) from 2023 to 2028, followed by energy and transportation (5%) and construction (2%) [5,7].

In the field of structural materials, composite materials exhibit substantial growth potential. Despite their current production volumes being lower than those of traditional materials, ongoing technological advancements offer significant opportunities to exploit this untapped potential.

2. Literature Review

2.1. Glass Fibers

Glass fiber remains the most widely used type globally [8], offering a favorable balance of mechanical performance and cost. E-glass fibers, the most common type, have a typical density of ~2.5 g/cm^3. The modulus of elasticity for glass fibers generally falls between 72 GPa and 85 GPa, depending on the type of fiber and the manufacturing process used [9,10].

Despite their beneficial properties, glass fibers pose significant manufacturing challenges. Their production consists of several critical stages, including high-temperature melting and precise fibrillation, which add to its overall complexity and energy demands [11]. These factors remain key limitations, even though glass fibers offer a favorable balance between mechanical performance and cost [12,13]. The intricate production process contributes significantly to the high energy consumption and associated CO_2 emissions, which are crucial indicators when assessing environmental impact. Compared to natural fibers, these environmental drawbacks represent a major disadvantage of glass fibers [14,15].

2.2. Resins

In the domain of matrices used in composite materials, the focus is primarily directed towards two categories of resins: thermoplastic and thermoset.

Thermoplastic resins are widely applied in the aerospace and automotive sectors, with prominent representatives including polypropylene (PP), polyamide (PA), and polyethylene (PE). These materials offer numerous advantages, such as high resistance, lightweight properties, affordability, and ease of handling. However, thermoplastics also have notable limitations, including a relatively low melting point and limited resistance to organic and polar solvents. Additionally, they are prone to permanent deformation and structural failure when subjected to continuous stress, such as cyclic loading or masticatory forces [16].

Thermoset resins are among the most extensively utilized systems in industries such as marine, construction, wind energy, aerospace, and consumer goods, including sports equipment. Key representatives of this category include polyesters, vinyl esters, epoxies, and phenolics. Similar to thermoplastics, thermosets are selected across these sectors based on their advantageous mechanical, physical, and technological properties [17,18].

Thermoset resins, such as epoxy or phenolic resin systems, offer superior mechanical properties compared to polyester and vinyl ester systems. However, these high-performance systems are typically associated with higher acquisition costs. To fully exploit their performance potential, fibers with enhanced mechanical characteristics, such as carbon or aramid, are often utilized. The most commonly used types for manufacturing epoxy systems are alkaline polycondensation products of epichlorohydrin and bisphenol A [19,20].

In recent years, bio-based epoxy resins have gained increasing attention due to their potential to reduce the environmental impact of resin production. These resins are derived partially or entirely from renewable or recycled sources, such as vegetable and soybean oils, lignin, tannins, and rosins [21]. Additional components may include saccharides, terpenes, cardanols, and syringaresinol, a naturally occurring, non-endocrine-disrupting bisphenol found in magnolia trees [22].

The main goal of these resins is to partially replace petrochemical components, with current commercial systems typically containing 25–60% bio-based content [19,23]. The literature suggests that, in developing these resins, it is essential to balance the proportion of bio-based components with the desired mechanical and technological properties of the final product [24,25]. These resins are particularly compatible with natural fiber reinforcements, which are gaining attention as sustainable alternatives to synthetic fibers.

2.3. Natural Fibers

Natural fibers, much like bio-based resins, are attracting increasing interest within the professional community. Studies suggest that natural fibers can be competitive with conventional glass fibers in terms of mechanical properties, such as the specific modulus of elasticity, thermal insulation, and acoustic insulation. In such instances, natural fibers may achieve comparable or even superior values compared to glass fibers [26–28]. The literature indicates that the cost of natural fibers can be up to 50% lower than that of widely used E-glass fibers. However, in some instances, natural fibers may exhibit higher costs. This variability arises from the diverse range of natural fiber types, variations in cultivation regions, and differences in the availability of surface treatment processes [29–33]. Furthermore, it is essential to consider variations in mechanical properties. Consequently, the cost of the amount of fibers required to achieve the same mechanical properties may, in certain cases, be comparable [29,34,35].

Although natural fibers typically have lower tensile strength than glass fibers, they offer benefits such as reduced density, biodegradability, and higher cost efficiency. Their natural origin reduces the carbon footprint through more sustainable sourcing and processing [35–37].

The literature emphasizes the importance of distinguishing fibers based on the nature of their source and the method of extraction, categorizing them into two types: primary and secondary plant fibers. The primary category refers to plants cultivated specifically for fiber extraction, such as jute, flax, hemp, and bamboo. The secondary category applies to plants where fiber extraction is a secondary process, typically involving the use of agricultural waste after harvesting the plant's fruits, as illustrated by banana plants, corn, or coconut [14].

After harvesting certain fruit species, about 60% of the biomass is left as waste. This can include pseudostems, which are abundant in cellulose fibers. These fibers are extracted through methods such as retting and mechanical separation, thereby utilizing what would otherwise be discarded as agricultural waste [38]. Natural fibers are organic materials derived from plants, animals, or minerals and are primarily composed of organic polymers.

The main component of plant fibers is cellulose, a polysaccharide that forms the structure of plant cells [39]. Cellulose is a long chain of glucose units connected by hydrogen bonds, providing the fiber with strength and durability. Plant fibers with a high cellulose content include flax, hemp, jute, bamboo, and sisal [40,41]. Other important components found in natural fibers are lignin and pectin. Lignin, an organic substance found mainly in woody fibers like those from hemp or bamboo, provides strength and resistance to environmental conditions. Pectins are polysaccharides that strengthen the cell walls of plants and are particularly abundant in fibers such as flax or apples [42].

Flax fibers, in particular, offer additional advantages, including the potential for cultivation across various regions of Europe [43]. However, flax fibers also present challenges, such as significant variability in mechanical properties and higher moisture absorption. Several studies have demonstrated that the hydrophilic nature of natural fibers causes them to absorb water in a humid environment and swell until saturation, which weakens

the bond between fibers and resin, potentially leading to a loss of mechanical properties and delamination [44–46].

A surface treatment is a possible solution to reduce moisture absorption. The most common methods include chemical treatment (alkaline, salinization or acetylation) and plasma treatment technologies. The literature confirms that chemical treatment of fibers can, in some cases, significantly reduce absorption depending on the chosen method [47,48]. Several technologies of plasma treatment can reduce fiber absorption and positively influence the mechanical properties of fibers [49–51]. An interesting alternative is the combination of chemical and plasma treatment, where natural fibers are first treated with plasma to remove hygroscopic components and enhance fiber wettability prior to subsequent chemical treatment [52]. Although plant fibers offer many advantages as an alternative to synthetic fibers, their hydrophilic nature necessitates a thorough understanding of their behavior in wet conditions before use [36]. Existing research consistently demonstrates that any surface treatment improves the mechanical properties of natural fiber composites; however, each additional technological step increases the production costs of fibers [53].

Natural fibers have densities ranging from 1.2 to 1.5 g/cm^3, with flax having a density of approximately 1.45 g/cm^3. The density can vary depending on the specific type of fiber. The modulus of elasticity for the most widely used flax fiber currently stands at 52.47 $\pm$ 8.57 GPa [29,54]. Hemp fibers can exhibit higher tensile strength compared to flax fibers, although both hemp and flax fibers have yielded varying results due to factors such as cultivation conditions, processing methods, and fiber characteristics [55]. However, the higher lignin content in hemp fibers makes them more challenging to process, as it contributes to increased stiffness. Additionally, hemp fibers are often more expensive than flax fibers, primarily due to the additional processing steps required to optimize their properties [56,57].

Mineral fibers, such as basalt, are gaining increasing recognition in multiple industries due to their unique properties and environmental benefits. Basalt fibers produce a product that combines ecological safety, long-lasting durability, and superior mechanical and chemical characteristics [58,59].

Numerous studies have demonstrated the potential of natural fibers in bio-composite structures, especially with regard to compliance with fire safety standards such as EN 45,545 [60]. Additionally, several investigations explore the use of natural fibers like flax or basalt in bio-based sandwich constructions, substituting recycled PET foams for conventional PVC as a more sustainable alternative [61].

2.4. Core Materials

Core materials are widely used in composite applications across various industries, including marine, aerospace, and construction. Their primary application is in structures subjected to high mechanical stress, where durability and strength are paramount. A broad range of core material types allows for optimization tailored to specific structural requirements [62,63]. For instance, honeycomb cores are available in cellulose-based materials, which are suitable for moderate stress applications, as well as in polymer-based honeycombs for structures that demand higher strength and durability. Among core materials in this sector, cellular foams are particularly prominent and are frequently used in composites reinforced with glass fibers and thermosetting resins [64].

In recent years, cellular foam composites have expanded into the energy sector, notably in wind turbine blade manufacturing, and are also widely used in the marine industry, forming the primary hull structures of recreational watercraft. Key types of cellular foam materials include PVC, PET, and PUR foams. These foams are manufactured through a controlled foaming process, where polyvinyl chloride (PVC) and polyurea are combined

with a foaming agent. The resulting product is typically shaped into slabs or blocks of constant thickness, ready for further processing. Heat forming is often required to produce consistent thickness and density, and these foams can be shaped using CNC machining or manual methods. For high-volume applications, injection molding can be used to produce foam cores, which can function as a prefabricated core insert for composite manufacturing [65].

A notable advantage of cellular foam materials is the extensive range of available thicknesses, formats, and densities. Foam density affects both mechanical performance and resin absorption; low-density foams show higher porosity, which may compromise structural integrity [66].

2.5. Balsa Core

The pursuit of environmentally responsible composite production has led to the exploration of balsa wood as a potential substitute for synthetic foam materials. Balsa (*Ochroma pyramidale*), a tropical tree species primarily native to South America, emerges as a promising alternative due to its low density (50–350 kg/m^3) and rapid growth rate [67,68]. The substantial variation in density can be attributed to the specific climatic conditions of the growth region. In the foreseeable future, demand for balsa as a core material in sandwich constructions is expected to increase.

Balsa cores are predominantly supplied in the form of board material, produced through a process in which individual balsa prisms are bonded together—typically using PVA glue—to form blocks that are then cut perpendicularly to the grain. Due to the natural variability in wood density, balsa boards are generally classified into three density categories: 80–120 kg/m^3, 120–180 kg/m^3, and 180 kg/m^3 and above. However, a significant drawback of these materials is the inconsistency in density even within classified groups. Consequently, a single prism of lower density can potentially determine the maximum mechanical properties of the slab, thus impacting the material's uniformity and predictability in performance [69].

2.6. Additive Manufacturing—3D Printing

Recent advancements in 3D printing—including improved hardware and a broader range of materials—have enabled its transition from home use to industrial applications [70,71]. Advancements are also reflected in the scaling of 3D printing equipment. Contemporary 3D centers now feature complex setups, such as robotic arms for both printing and surface finishing [72]. A major challenge within additive manufacturing remains the integration of cellular foams with 3D printing technologies. This study explores challenges and innovations involved in producing foam materials through additive manufacturing processes [73].

In the field of composite manufacturing, 3D printing, or additive manufacturing, is widely used for model making, rapid prototyping, and mold production for final products, with fused deposition modeling (FDM) being the most prevalent technique [74]. Recent research has also explored the use of 3D-printed structures as sacrificial absorbers or as adaptive mechanical components. In combination with thin-walled laminates, these components can function as dynamic systems, such as adjustable wings [75,76].

Another notable innovation in additive manufacturing and composite materials is a technology where continuous synthetic fiber is printed together with thermoplastic material using a 3D printer [77]. This approach enhances mechanical properties and expands the applications of 3D-printed structures in high-performance industries.

The use of 3D printing in construction is gaining attention for its efficiency, ability to address unconventional challenges, and cost reduction in residential development [78–80].

Research focuses not only on automated construction processes but also on novel materials, particularly cementitious and concrete-based composites [81–84]. Recently, studies have explored thermoplastic printed cores inspired by honeycomb structures to enhance the mechanical properties of sandwich panels. However, their performance largely depends on proper design [85,86].

The literature suggests that, in certain cases, three-point bending tests indicate that a rhombus core exhibits higher stiffness than a honeycomb core. This behavior is attributed to the rhombus core's lower proportion of angular components in the loading direction and its stronger reinforcement effect in the perpendicular direction. Experimental results confirm that the mechanical behavior of sandwich structures is significantly affected by core geometry, where design optimization through 3D printing can enhance strength and stiffness [87,88]. However, the measured tensile strength and modulus of elasticity were lower than predicted, likely due to defects introduced during the printing process and discontinuities such as fiber gaps. Consequently, 3D-printed sandwich structures demonstrate reduced mechanical resistance compared to conventionally manufactured CFRP panels [89,90]. These findings underscore the need for further research aimed at process optimization and geometric refinement to fully leverage the advantages of additive manufacturing in the design of structural composites.

The increasing integration of 3D printing in composite manufacturing presents opportunities to tailor core geometry and material distribution. This study compares sandwich structures with conventional and 3D-printed cores, focusing on mechanical performance, density, and sustainability. The core contribution lies in evaluating the potential of 3D-printed cores as viable alternatives to traditional solutions and, in some cases, as superior ones. Through parametric modeling and additive manufacturing, the study demonstrates how design flexibility enables application-specific geometries optimized for targeted loading conditions. This adaptability also supports reverse-engineering strategies to refine core architecture and improve structural efficiency.

A novel aspect of this study is the experimental evaluation of a scarcely explored material system: 3D-printed thermoplastic cores reinforced with natural fibers. This unique integration demonstrates competitive mechanical properties and offers a pathway to fully or partially sustainable sandwich composites. By combining the design freedom of additive manufacturing with renewable reinforcements, this approach enables lightweight, customizable, and environmentally conscious structures, which is an area largely unexplored in the existing literature.

3. Materials and Methods

3.1. Materials

Four groups with different fiber reinforcements and core materials were produced, with each group containing 10 samples. For mechanical testing, sample dimensions were standardized at 50 × 290 × 12 mm, while density profile measurements utilized samples measuring 50 × 50 × 12 mm (Figure 1).

The GF group was constructed using two outer layers of Aeroglass 200 g/m^2 twill fabric (Havel Composites, Svésedlice, Czech Republic) from each side with a PVC foam core of 110 kg/m^3 density (3A Composites, Sins, Switzerland).

The FF group was similarly produced with the same PVC foam core as the GF group but reinforced with two layers of flax fiber (FLAXDRY-BL200 200 g/m^2 twill fabric; EcoTechnilin, Valliquerville, France).

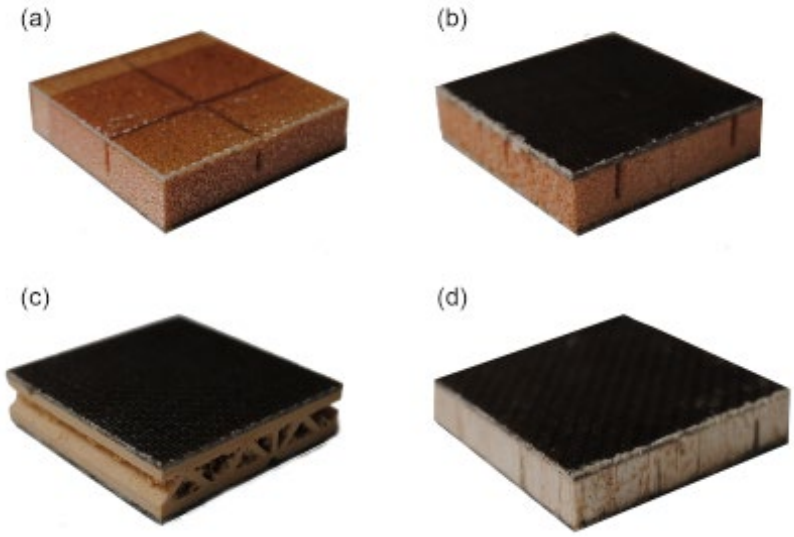

Figure 1. Samples cross section of groups (**a**) GF group, (**b**) FF group, (**c**) F3D group, and (**d**) FB group.

For the F3D group, the core material consisted of a 3D-printed structure using foaming polylactic acid (PolyLight 1.0 LW-PLA; 3D LabPrint, Brno, Czech Republic) [91]. The FB group utilized an end-grain balsa core with a density of 150 kg/m^3 (Easy Composites Ltd., Longton, UK). Table 1 outlines the grouping and material composition of sandwich structures for clarity in abbreviation usage.

Table 1. Composition of sandwich structure groups.

Group	Fiber	Core
GF	Aeroglass 200 g/m^2 twill	PVC core foam
FF	FLAXDRY-BL200 200 g/m^2	PVC core foam
F3D	FLAXDRY-BL200 200 g/m^2	PolyLight 1.0 LW-PLA
FB	FLAXDRY-BL200 200 g/m^2	End-grain balsa core

All samples were infused with IB2 Epoxy Infusion Bio Resin (Easy Composites Ltd., Longton, UK), a high-performance bio-based epoxy system specifically designed for advanced resin infusion applications. With a viscosity of 185 mPa·s at 25 °C, it ensures optimal fiber wetting and minimizes void content in composite structures.

The 3D-printed core (intended thickness: 10 mm) and the balsa core (measured thickness: 9.5 mm) were both close to their respective target thicknesses of 10 mm and 12 mm. The selected geometry for the 3D-printed core, resembling a truss structure, was chosen based on material-specific considerations. Due to foaming additives in the thermoplastic material, the printing parameters required adjustment.

PolyLight 1.0 LW-PLA (3D LabPrint, Brno, Czech Republic) is a lightweight foaming PLA filament designed for weight-sensitive applications. Utilizing active foaming technology, it expands when heated, reducing its density from 1.24 g/cm^3 to approximately 0.54 g/cm^3 within a print temperature range of 215–250 °C. Higher nozzle temperatures increased surface porosity, while lower temperatures led to reduced porosity.

Unlike conventional thermoplastic materials commonly studied in current research [88,90], foaming-grade polymers undergo thermal expansion within the nozzle, disrupting standard operations such as filament retraction and causing surface defects like stringing [92,93]. Excessive foaming at elevated temperatures exacerbates these issues and may introduce impurities that reduce mechanical performance. A printing temperature of 240 °C was

identified as optimal for balancing foam quality and process stability. To further minimize defects, strategies such as continuous extrusion paths, similar to "vase mode", can reduce retractions. Comparable extrusion-related challenges have also been reported in functional materials, including self-healing polymers [94].

Given these considerations, the standard infill strategy commonly used in the literature was not applied in this study. Instead, a customized approach optimized for foaming materials was implemented to improve print quality and process reliability. PVC foam showed slightly higher average thickness (measured at 10.5 mm), influencing the final sample thickness, which averaged 12 mm. Some specimens in this group reached thicknesses up to 12.5 mm.

The test samples were produced using vacuum infusion technology. Samples were fabricated on 6 mm tempered glass, which was pre-cleaned with Sea-Line cleaner and degreaser. The glass surface was subsequently waxed with Oskar's M700/C (Oskar's GmbH, Karlsruhe, Germany), and eight layers of release agent were applied according to the technical data sheet instructions. Two layers of 200 g/m^2 twill fabric were placed on the outer surfaces, sandwiching the dry core between them. A 105 g/m^2 peel-ply fabric was applied to the visible side of each sample, and each sample was then hermetically sealed with vacuum film. Vacuum was applied using an EC4 Compact Composites Vacuum Pump, supplemented with a VR20 vacuum controller and VF1 air filtration system. After vacuuming the dry samples, a full seal test was conducted by closing the valves for 1 h and measuring any vacuum drop in the system. All samples were infused under full vacuum, with PVC tubing (6 mm internal cross-section) used to distribute the resin evenly.

3.2. Methods

Each sample was weighed and measured across all three dimensions (X, Y, and Z) to calculate bulk density. The density profile of each sample was determined using the IMAL DPX300 LTE X-ray density profile analyzer (Imal-pal Group, San Damaso, Italy). Measurements were conducted on five individual samples from each group, with data from each sample plotted on a linear graph. The calculated density values for each sample are presented in Table 1.

Bending characteristics were evaluated using the TIRA Test 2850 machine (TIRA GmbH, Schalkau, Germany) in compliance with EN 310 (1995) standards. The modulus of elasticity in bending and the bending strength were determined by applying a central load to each specimen, which was supported at two distinct points.

Figure 2a illustrates the bending test of a sample made with flax fiber composite and a 3D-printed core structure, while Figure 2b shows the density profile measurement procedure using the IMAL DPX300 LTE densitometer.

Figure 2. (**a**) Bending test on TIRA test 2850; (**b**) measurement procedure by IMAL DPX300 LTE.

The calculations for the modulus of elasticity, denoted as E_m, and the bending strength, represented as f_m, were conducted utilizing the subsequent Equations (1) and (2).

$$E_m = \frac{(F_2 - F_1)l_1^3}{4bt^3(a_2 - a_1)} \quad (1)$$

$$f_m = \frac{3F_{max}\, l_1}{2bt^2} \quad (2)$$

where l_1 is the distance between the centers of the supports [mm], b represents the width of tested pieces [mm], t is the thickness of the test samples [mm], and $F_2 - F_1$ is the load increment within the linear portion of the load–deflection curve [N]. F_1 might be approximately 10% and F_2 approximately 40% of the maximal load. $a_2 - a_1$ is the increment of deflection at the mid-length of the specimen [m]. F_{max} is the maximal load [N].

Fracture surfaces of the test specimens were evaluated visually and with a ZEISS Axio Zoom V16 digital light microscope (Carl Zeiss Microscopy GmbH, Jena, Germany) at various magnifications. The Axio Vision SE64 software 4.9.1. (Carl Zeiss Microscopy GmbH, Jena, Germany) was used for detailed examination of the interfacial regions between the epoxy matrix and reinforcing fibers as well as the core of the composite panel.

Overview images were captured using the ZEISS Apo Z 1.5x/0.37 FWD 30 mm objective and the Extended Depth of Focus (EDOF) function. The final images were composed from a series of approximately 100 individual frames acquired at 10 µm increments. The EDOF function was employed to ensure a consistently sharp image across the entire depth of the examined region by computationally merging images captured at different focal planes.

Measured values from mechanical tests were analyzed in MS Excel to calculate the mean ($\bar{x}$), minimum, maximum, and standard deviation (SD) for each group. The resulting data were visualized using basic statistical tables and graphs. Box-whisker plots were employed to represent the mechanical properties, illustrating mean values, quartiles, and data points deviating from the main distribution. These deviations were categorized as outliers, defined as values lying beyond 1.5 times the interquartile range (IQR), and extreme values, which significantly deviate beyond the typical range, exceeding 3 times the IQR.

Statistical differences between groups were evaluated using analysis of variance (ANOVA) followed by Tukey's honest significant difference (HSD) test at a significance level of $\alpha = 0.05$. All statistical analyses were conducted using Statistica software (version 13, TIBCO, Santa Clara, CA, USA).

4. Results

4.1. Density Profile

The density of the produced samples was calculated and is summarized in Table 2. Group GF exhibited an average density of 416.56 kg/m^3. Group FF showed a density approximately 3% higher than group GF, representing the highest value overall. Group F3D had an average density of 424.46 kg/m^3, while group FB recorded the lowest average density at 405.41 kg/m^3.

Table 2. Density parameters for sample groups.

Group/Sample	$\bar{x}$ [kg/m^3]	Min [kg/m^3]	Max [kg/m^3]	SD [kg/m^3]
GF	416.56	399.96	437.22	15.77
FF	432.21	416.88	447.56	12.83
F3D	424.46	396.73	440.76	17.63
FB	405.41	384.93	431.86	18.29

The data reveal the density profile of the clusters as measured by the IMAL DPX300 LTE density profile analyzer (Figure 3). The density profile for each group is derived from the mean measurements of all test specimens within the respective group. In each profile, the smooth side of the test specimens, which contacted the separated surface during production, is consistently denoted by a value of 0 on the *X*-axis, while the maximum *X*-axis value corresponds to the side where solid infusion occurred.

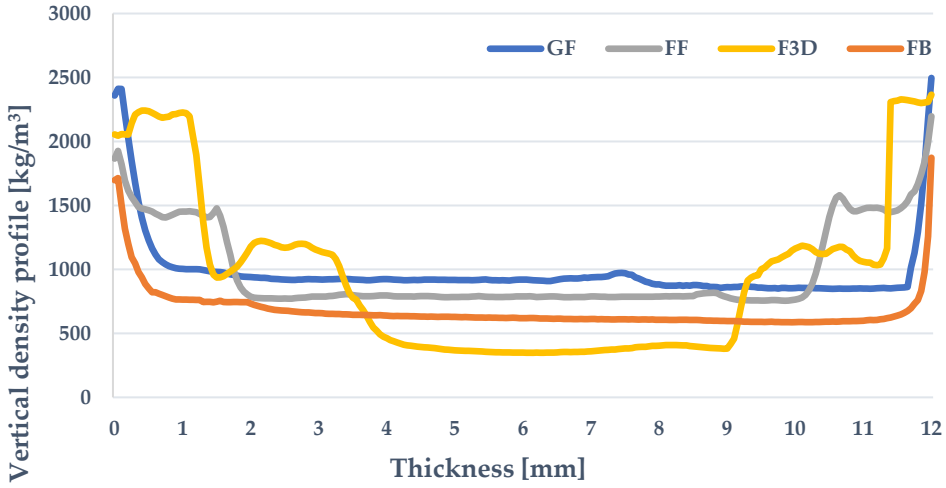

Figure 3. Representation of the results of density profile measurements of groups using the IMAL DPX300 LTE density profile analyzer.

The curves reveal discrepancies between theoretical bulk densities and measured profiles. Across all groups, a characteristic distribution is evident, with high density observed in the outer layers and markedly lower density in the core regions of the sandwich material.

The GF group demonstrated the most distinct pattern, with its density profile showing a consistent linear decrease and subsequent increase at comparable values along the *X*-axis. In this group, the PVC foam core density measures approximately 900 kg/m^3, while the measured density of the raw Airex foam is 110 kg/m^3. The density of the raw core is influenced by the presence of the PP grid and groove patterns, which facilitate foam absorption, potentially increasing the core density by up to 818%. A similar effect was observed in the FF group samples, though the foam absorbed a reduced amount of resin, resulting in a core density increase of only 690% relative to the raw material.

This substantial increase in core density is attributed not only to resin absorption but also to the presence of resin within grooves in the core that enhance resin distribution during the manufacturing process. According to the technical data sheet, the density of the epoxy resin matrix used is 1100 kg/m^3.

The experimental results indicate that the foam core achieved the highest density among all tested groups. Specifically, the density profile remained stable, with the outer layers—reinforced by glass fibers—exhibiting the highest density, while the middle section of the structure displayed the lowest density. Notably, the foam core itself showed a higher density compared to the cores of other groups.

One of the main objectives of sandwich structures is to reduce the product's weight while simultaneously enhancing its mechanical properties or achieving the same mechanical properties as products made, for instance, from solid laminate but with the benefit of reduced weight. Foam cores, despite their high absorbency, can achieve such results. However, future research could focus on the trade-off between increased core density

and its influence on mechanical properties. Increased core density positively impacts the mechanical performance of the entire structure.

The FF group exhibited a comparable density profile, with the outer layers displaying the highest density and the core presenting the lowest. However, both the core and outer layers in the FF group exhibited lower densities than those observed in the GF group. Data analysis indicates that the foam core density is influenced by resin absorption at the fiber/foam interface. Flax fibers demonstrated higher matrix absorption, which may lead to resin uptake from the sandwich core during the production process.

The F3D group showed a typical density profile for sandwich structures, albeit with greater variability in density values within the transition region between the reinforcement layers and the 3D-printed core. The lowest density measured across all groups occurred within the deeper sections of the structure, approximately in the thickness range of 4 to 9 mm, suggesting deeper matrix penetration in this inter-transition region. This variability in the density profile of the 3D-printed core may be attributed to differences in the geometry of the infill material across samples.

The FB group demonstrated a similar density profile but lacks the density variability observed at the fiber-core interface, indicating that balsa does not possess the same absorption properties as foam materials, and the resin does not infiltrate the material's pores. This difference may be influenced by the surface characteristics of the core materials; foam cores, with their inherently more porous surfaces, likely facilitate greater resin absorption compared to the smoother, less porous surface of balsa cores.

The measured data also support previous research [35], showing that in all cases of groups containing flax fibers, lower density values were achieved in the outer layers than in the GF group containing glass fibers. Despite the higher absorption capacity of flax fibers relative to synthetic fibers, the overall density of the reinforcement remained lower. This phenomenon is further supported by the fact that glass fibers exhibit significantly higher density values compared with natural fibers.

4.2. Modulus of Elasticity

Table 3 confirms that glass fibers yield the highest modulus of elasticity among all tested reinforcements. Specifically, the GF group recorded an average modulus of elasticity of 5085.12 MPa, with individual measurements ranging from 4914.52 MPa to 5409.55 MPa. In contrast, the FF group demonstrated an average modulus of elasticity that was 47% lower than that of the GF group, corroborating current research [95,96] indicating that glass fiber composites generally achieve superior mechanical properties compared to any alternatives such as natural fibers or any hybrid options. The F3D group exhibited an average modulus of elasticity of 2269.19 MPa, reflecting a modest reduction in performance of only 6.6% relative to the FF group, which also utilized flax fiber. Meanwhile, the FB group achieved an average modulus of elasticity of 2445.25 MPa, marking it as the highest among groups containing flax fiber and the second highest across all tested groups.

Table 3. Measured data of modulus of elasticity, regardless of samples orientation.

Group	$\bar{x}$ [MPa]	Min [MPa]	Max [MPa]	SD [MPa]
GF	5085.12	4914.52	5409.55	175.31
FF	2429.28	2120.85	2971.30	254.24
F3D	2269.19	2216.60	2310.52	29.93
FB	2445.25	2196.85	2782.82	193.40

The modulus of elasticity associated with the core materials indicates that the three tested core types yielded comparable values when paired with the same fiber reinforcement (Figure 4). Specifically, the balsa core demonstrated an average modulus of 2445.25 MPa, closely followed by the PVC core with an average of 2429.28 MPa (FF group), and the 3D-printed core with an average of 2269.19 MPa. Notably, the PVC core exhibited enhanced performance when combined with the GF group, which incorporates glass fiber reinforcement. This pairing significantly strengthens the mechanical properties of the PVC core, providing increased rigidity and strength due to the reinforcing effect of the glass fibers.

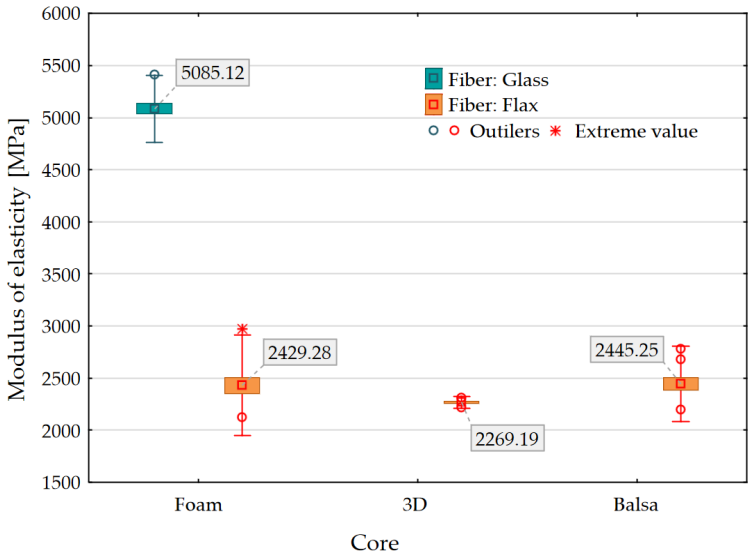

Figure 4. Modulus of elasticity related to the core material, categorized by fiber. The graph displays the mean value, with boxes representing the lower and upper quartiles and vertical bars indicating the non-outlier range.

In the GF group, distinct differences in modulus of elasticity were observed based on the orientation of the foam handling and infusion grooves (Figure 5). Specifically, specimens tested with the grooves oriented upwards exhibited a 3.9% higher average modulus of elasticity (5184.80 MPa) compared to specimens with grooves oriented downwards (4985.43 MPa). This trend is reflected in the variation range for the upward orientation, with the maximum recorded value reaching 5409.55 MPa and the minimum at 4914.52 MPa. In contrast, the highest observed modulus in the downward-oriented samples was 5027.79 MPa. These variations may be attributed to the resin distribution within the grooves; when the grooves are oriented upwards, the resin is subjected to compressive stress, potentially creating favorable loading conditions that enhance the structural performance.

Using Tukey's HSD test, it was determined that the modulus of elasticity results for the GF group differed statistically significantly from all other groups (p = 0.000138 and p = 0.000180 for the upwards and downwards orientations, respectively). No statistically significant differences were observed among the other groups.

An intriguing observation emerged in the comparison between the GF and FF groups. In the FF group, specimens with grooves oriented upwards exhibited lower modulus of elasticity values, averaging 2286.56 MPa. Conversely, specimens tested with downward-oriented grooves achieved values that were 11.1% higher, with an average of 2571.99 MPa. These results imply that the absence of resin within the grooves of the FF group, likely due to increased absorption by the flax reinforcement, resulted in air gaps that did not contribute to compressive strength enhancement as observed in the GF group.

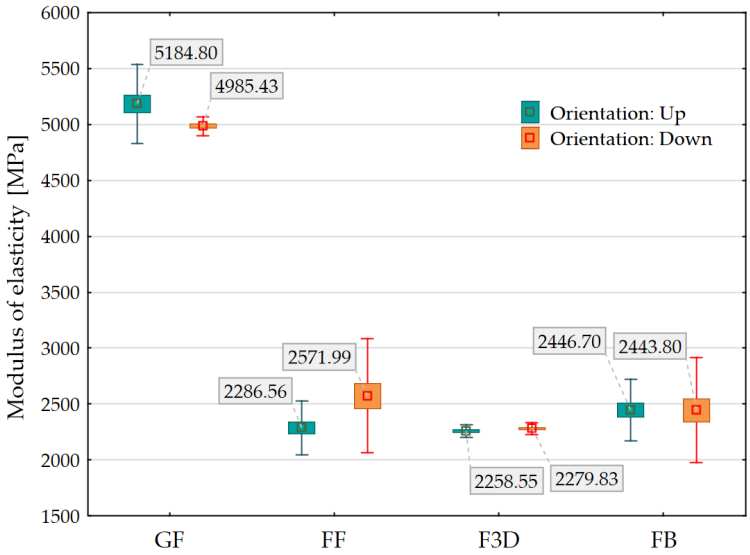

Figure 5. Modulus of elasticity, categorized by orientation of samples during the test.

Samples from the FF group demonstrated that producing a panel with the same natural fiber weight and foam core as in the GF group, which utilizes synthetic fibers, requires a greater amount of resin to achieve adequate saturation. The resin absorbed by the core represents an undesirable effect and corroborates findings in the literature, which indicate that natural fibers demand more resin than synthetic fibers [97,98].

A viable solution to this issue might involve optimizing the infusion process, such as reducing the infusion rate by modifying the resin viscosity, thereby ensuring complete and uniform saturation of both the fibers and the core. Another approach, as highlighted in the literature [99], could involve advancing research in natural fiber surface treatment to evaluate commonly used protection methods and their effects on moisture and resin absorption. Finally, the possibility of incorporating additives into the resin prior to the manufacturing process warrants consideration. This approach has been shown to modify the matrix, enhancing resistance to biotic factors or improving abrasion resistance [100]. Addressing these challenges will be a key focus of future research.

The application of identical conditions for all sample groups in this study ensured a valid comparison between groups. It can be concluded that the design of a structural element with a foam core must account not only for the shape of the element but also, in the case of infusion technology, for the orientation of the foam and the distribution channels facilitating resin flow. Fully saturated channels contribute to an increase in the overall weight of the structure; however, they also enhance its strength. This enhancement occurs because the top layer of the structure experiences compressive loading in contrast to the tensile stresses on the bottom layer.

For the F3D and FB groups, the orientation of specimens during testing appeared to have negligible influence on the measured values, with the F3D group, in particular, displaying exceptional consistency in its results. The overlapping variation ranges among all groups support the conclusion that their mechanical properties are highly comparable. Moreover, examining these values alongside the density profiles of each group yielded additional insights. Despite showing the lowest average modulus of elasticity, the 3D-printed core group exhibited one of the highest density profiles among the tested samples. However, the 3D-printed core material showed the lowest density overall according to the density profile.

The PVC foam core groups demonstrated intermediate modulus values, achieving the highest density profile when used with flax fiber reinforcement. The modulus of elasticity

for the 3D-printed core was specifically measured along the primary direction of the filler to capture the structure's lowest possible modulus values. In contrast, the other groups, due to the intrinsic nature of their materials, exhibited uniform properties across the X- and Y-axes.

4.3. Bending Strength

The GF group, with a bending strength of 43.88 MPa (Table 4), is only 14% higher than the FF group and 42% higher than the FB group (30.83 MPa). Interestingly, in certain cases, samples from the FF group, which recorded the lowest values in modulus of elasticity, achieved comparatively higher bending strength (Figure 6).

Table 4. Measured data of bending strength related to groups, regardless of samples orientation.

Group	$\bar{x}$ [MPa]	Min [MPa]	Max [MPa]	SD [MPa]
GF	43.88	34.52	54.40	8.67
FF	38.41	31.24	48.01	5.63
F3D	31.46	29.17	34.62	2.01
FB	30.83	20.72	37.04	5.68

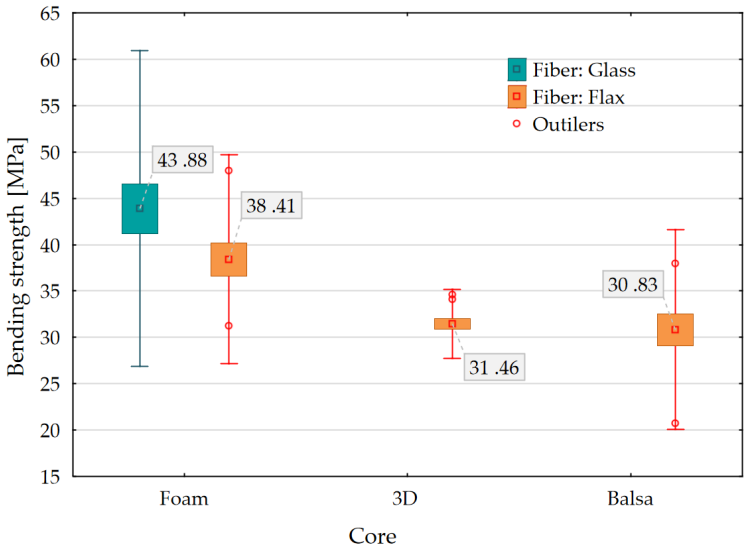

Figure 6. Bending strength of samples categorized by core.

The F3D group exhibited the smallest variation in its measured bending strength data, aligning with previous findings on the modulus of elasticity for this group and indicating a high degree of consistency in its mechanical properties. The maximum recorded bending strength for the F3D group was 34.62 MPa. Although this value does not reach the performance levels observed in the GF group—where the lowest bending strength recorded is 34.52 MPa—it remains within the lower range of the values measured for the FF group, underscoring the moderate performance of the F3D configuration.

An analysis of the bending strength data across all groups revealed that flax fibers attain their highest values when combined with a PVC foam core, reaching 38.41 MPa. This is followed by the F3D group, where flax fibers were paired with a 3D-printed core, resulting in an average bending strength of 31.46 MPa. Meanwhile, the combination of flax with a balsa core yielded an average bending strength of 30.83 MPa, which is only 0.57% lower than the F3D group. These findings highlight the influence of core material on the structural performance of flax fiber composites. PVC foam provided the highest

reinforcement effect, while the 3D-printed core and balsa core configurations demonstrated competitive yet slightly lower bending strength values.

As anticipated, the highest bending strength (Figure 7) was observed in the GF group when samples were oriented with the grooves facing upward during testing, a trend consistent across both orientations within the group. A similar trend was noted in the FF group, although its bending strength values were 18.5% lower at 42.22 MPa compared to the GF group. In contrast, similar to the modulus of elasticity results, the orientation of the samples during mechanical testing did not have a significant impact on the bending strength measurements for the F3D and FB groups.

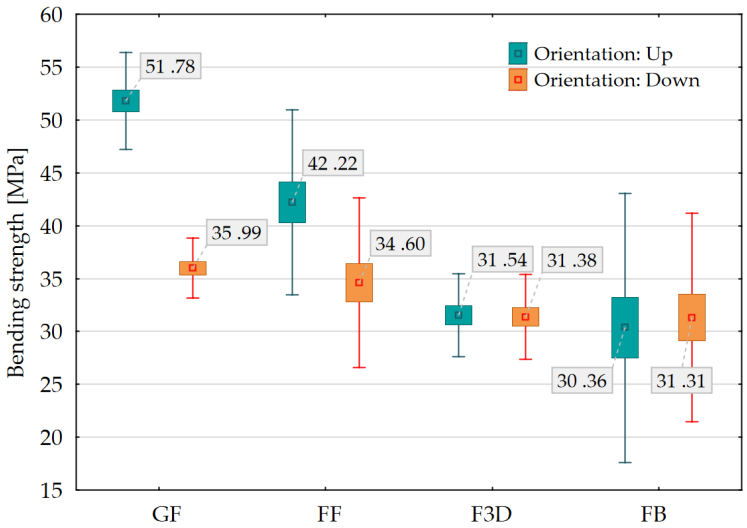

Figure 7. Bending strength of measured groups, categorized by orientation of samples during the test.

The F3D group exhibited a 25.3% reduction in performance compared to the FF group when samples were oriented with grooves facing upwards. However, with a downward orientation, the reduction in the F3D group's values was only 8.8%, and in comparison to the GF group, the decrease was 12.4%. This discrepancy may be attributed to the F3D group's homogeneous and consistent cross-sectional shape, which lacks the resin infusion channels present in other core configurations.

The FB group, with a balsa core, exhibited performance values 31% lower than the GF group and 21% lower than the FF group yet remained within the acceptable variation range. The F3D group displayed mechanical properties comparable to the FB group, with overlapping ranges observed with the FF group. Additionally, the F3D group showed significantly smaller variance in performance compared to the other groups, indicating greater consistency. The results of Tukey's HSD test showed p-values exceeding the significance level ($p > 0.05$) for all groups except GF upwards, indicating that the observed differences between the tested samples were statistically insignificant. These findings suggest very similar strength values across the groups, with the exception of GF, which exhibited significantly higher strength.

The results of the conducted measurements support previous research in this field, demonstrating that 3D-printed core structures have the potential to serve as a viable alternative to conventional core materials [101]. The existing literature highlights that the geometric configuration of the 3D core infill and its density are critical factors that significantly influence the mechanical properties of the overall structure. Therefore, further research in this area is strongly recommended [85].

The success of sandwich structures depends on achieving an optimal balance between the core's geometry and porosity, the type of fiber and its absorbency, and the resin's viscosity, all of which must be optimized for the manufacturing process. The epoxy resin used in sample production exhibited low viscosity, as specified by its technical parameters. However, alternative resin systems with even lower viscosities are available on the market, potentially offering improved fiber wettability in certain cases.

Additionally, it is important to highlight that the selected resin system contains 35% bio-based content, a level that infusion resin systems do not always achieve. The development of this technology holds great promise for applications not only in construction but also in engineering.

Parametric modeling allows for the optimization of both the shape and properties of the outer layers and core of sandwich structures. Until now, this level of customization and optimization has not been possible with conventional core materials, which often do not allow the same level of design flexibility and precision achievable through 3D printing. Recent studies confirm our hypothesis that combining conventional manufacturing processes with advanced 3D printing technologies, such as carbon fiber printing, can yield promising results [102].

Traditional materials struggle to offer the same level of design adaptability and performance enhancement. In contrast, 3D printing technology enables easy core modifications, allowing for tailored designs to meet specific requirements. As a result, the continuous optimization of the 3D-printed core and outer layers remains a central focus of ongoing research.

4.4. Failure Modes

In the GF group samples, a typical brittle fracture in the outer layer under tensile stress was observed. The load-deflection diagram in Figure 8 indicates that brittle fracture occurs with almost no plastic deformation of the material. The fracture surface is characteristically smooth and glossy.

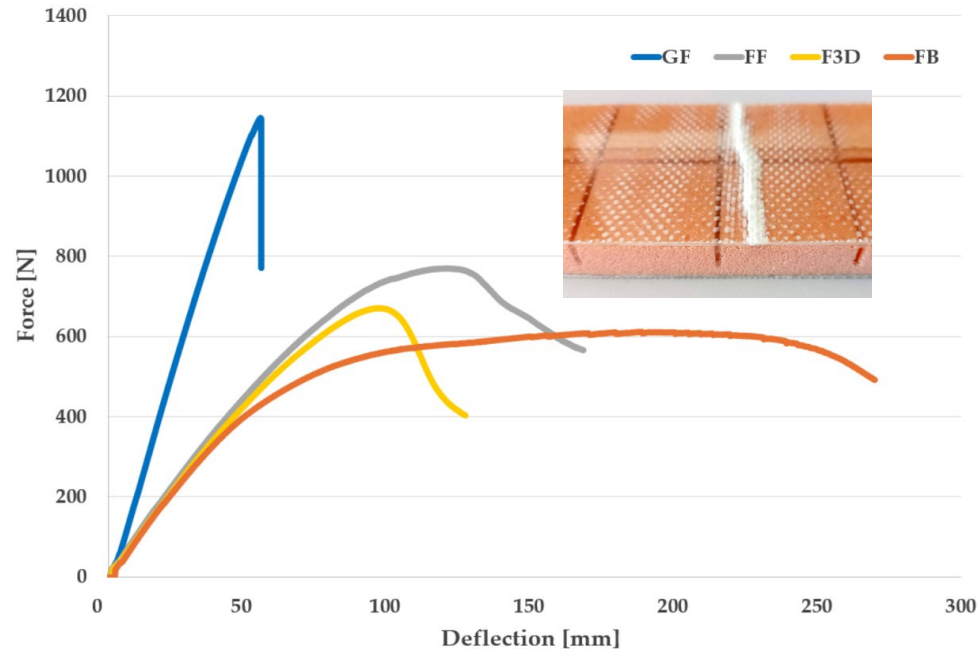

Figure 8. Load–deflection diagrams. For each group, plots representing samples with average values were selected. The graph also includes a detailed image of a sample from the GF group after testing.

In the FF group, various types of fractures were observed. A significant factor influencing the fracture type was the orientation of the sample during testing. Samples tested with the smooth side oriented downward predominantly exhibited a mixed-mode failure, involving core compression failure and face layer delamination. The low resin saturation of the foam core likely contributed to the reduced mechanical properties observed in this group. Conversely, samples with the smooth side oriented upward primarily displayed a mixed-mode failure, characterized by core compression failure or brittle fracture.

The F3D group displayed consistent fracture patterns across all samples. In most cases, this involved core shear failure or core compression failure of the 3D-printed core. It can be inferred that the designed infill of the printed core deformed either due to exceeding shear strength or because of the core's low density and strength. Deformation or collapse of the core was visible directly under the loading point, which is a typical failure pattern for honeycomb cores [103].

In the FB group, as in the GF group, brittle fracture predominated. From the load-deflection diagram and observations of the samples after mechanical testing, it is clear that, after the failure of the outer tensile layer, the load was transferred to the balsa core until its load-bearing capacity was exhausted. Similar patterns were observed across all samples within the group, regardless of their orientation during the measurements. The literature suggests [104] that the mechanical properties of balsa wood are significantly influenced by its microstructure, which may lead to behavior distinct from that of conventional core materials.

4.5. Microscopic Analysis

Figure 9a–d present the fracture surfaces of individual specimen groups after the bending test. The images provide a detailed view of the bottom side of the specimen, where tensile failure occurred due to the applied loading. This region is critical for analyzing the fracture mechanisms, including fiber breakage, matrix cracking, and interfacial debonding, which contribute to the overall failure behavior of the composite material.

The fracture surface of glass fibers was typically smoother, with pronounced fiber fragmentation and splitting, whereas flax fibers exhibited a more ductile fracture, characterized by fibrous and progressive detachment, partial fiber pull-out, or even the extraction of entire fiber bundles from the fabric.

The microscopic analysis of the GF group samples indicates that the resin fully permeated the cross-section, saturating not only the outer layer but also the foam core throughout its entire depth. This extensive saturation ensures strong adhesion between the outer layer and the core. However, it also increases core density, which, while beneficial for mechanical performance, results in a higher overall structural mass.

Conversely, in the FF group, incomplete saturation of the foam core was observed, while the flax fiber outer layer exhibited increased thickness. This phenomenon can be attributed to the high absorbency of flax fibers, which retained a substantial amount of resin during the manufacturing process. This behavior led to reduced adhesion at the interface between the outer layer and the core, thereby diminishing the mechanical performance of the composite. Microscopic analysis confirmed the previously observed delamination in a larger number of samples.

For the F3D samples, the core exhibited limited resin penetration, with significant absorption occurring within the outer flax layer, similar to the FF group. In some F3D samples, signs of delamination were observed, likely due to insufficient adhesion between the minimally penetrated core and the outer layer. This issue could potentially be mitigated by optimizing 3D printing parameters, such as printing a textured surface on the 3D-printed core, and by adjusting core manufacturing settings to enhance interfacial bonding.

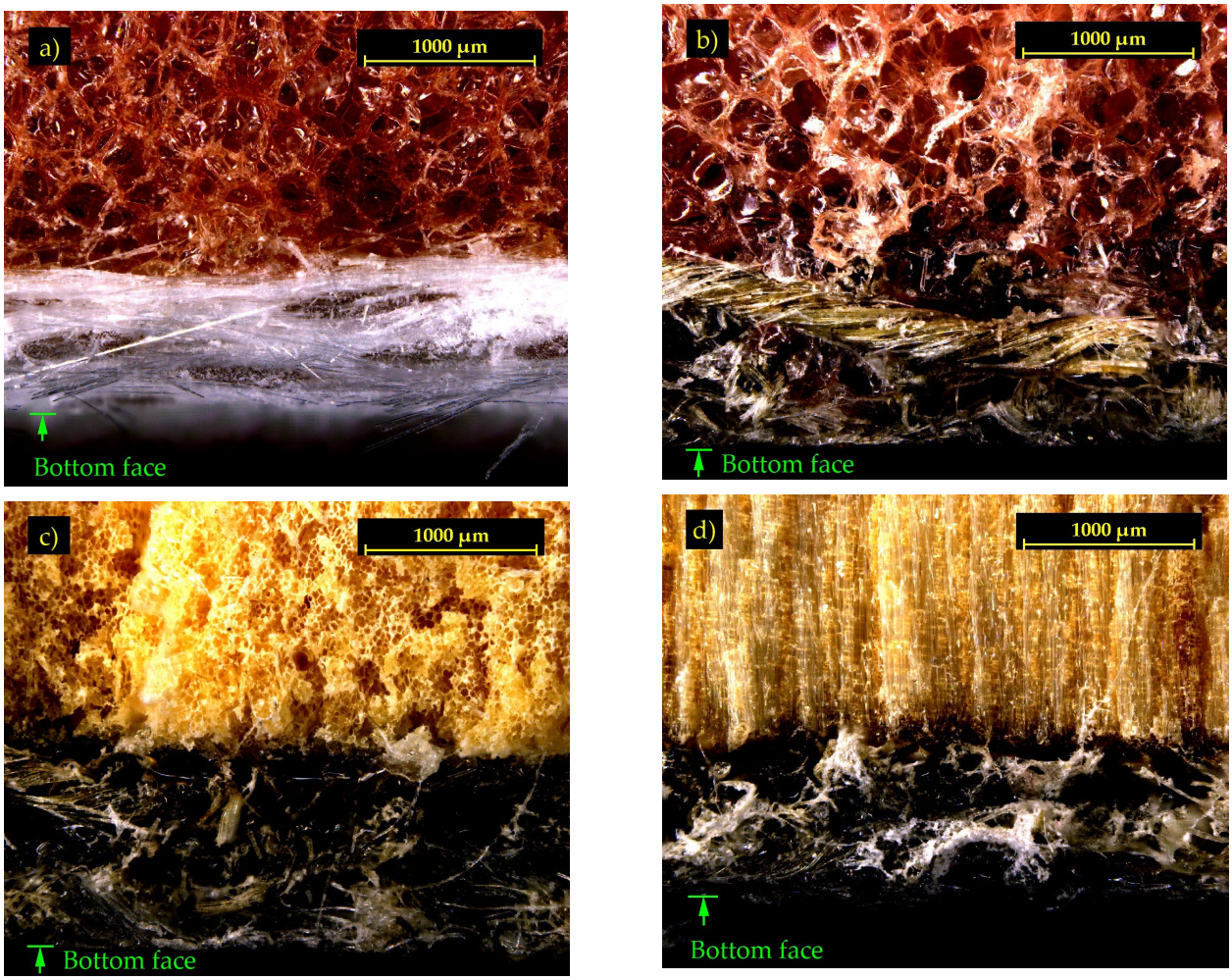

Figure 9. Fracture surface images for individual specimen groups: (**a**) GF group, (**b**) FF group, (**c**) F3D group, and (**d**) FB group.

The FB sample analysis revealed that, despite the relatively low porosity of balsa wood, significant resin infiltration into the core occurred. Compared to other flax fiber-based groups, the outer layer was thinner, indicating resin penetration into the balsa. However, frequent delamination occurred, likely due to low surface porosity and the presence of microcracks, which led to uneven resin distribution.

Previous research [105–107] confirms that core porosity and density significantly influence mechanical properties. A sufficiently porous core enhances resin absorption and bonding, as observed in the GF group, whereas less porous surfaces, such as in the FB group, increase the risk of delamination under mechanical stress.

The F3D group, with intermediate density and porosity, limits resin penetration while effectively preventing delamination. Unlike conventional materials, 3D printing allows systematic control over these characteristics by adjusting printing parameters and surface texture, optimizing resin distribution and adhesion while maintaining low density. Future research will focus on 3D printing parameter optimization and process refinement to enhance core properties.

5. Conclusions

Experimental results confirm that both natural and 3D-printed core materials are viable alternatives to traditional sandwich cores, providing favorable mechanical and density characteristics for structural applications.

- Glass fiber reinforcements achieved superior mechanical properties compared to flax fibers, including higher tensile strength and greater stiffness;
- Flax fiber reinforcement reduced impregnation efficiency in foam cores, negatively affecting certain mechanical characteristics;
- Although flax fibers absorbed more resin, they maintained a significantly lower density than glass fibers;
- Despite their lower mechanical performance, flax fibers provide an environmentally friendly alternative, making them suitable for sustainable composite production;
- Density profile measurements showed that the 3D-printed core had the lowest raw material density yet delivered comparable performance in selected tests. In the F3D group, the resulting composite density was intermediate among flax-reinforced samples;
- Mechanical testing confirmed that lightweight 3D-printed thermoplastic cores can match the performance of conventional foam and balsa cores. Moreover, 3D-printed materials exhibited greater consistency and homogeneity in their properties;
- The modulus of elasticity for samples with 3D-printed cores averaged 2269.19 MPa, with statistical analysis revealing overlapping values with groups utilizing conventional core materials.

While slightly lower in peak mechanical performance, 3D-printed cores offer considerable freedom in structural design. Their geometry, density, and internal architecture can be tailored to specific application requirements, enabling optimization beyond the limitations of conventional core materials.

This study contributes to the emerging field of digitally tailored composites by experimentally validating that lightweight thermoplastic cores, particularly in combination with natural fiber reinforcement, can deliver competitive mechanical performance. In addition, they offer notable advantages in terms of sustainability and adaptability in the manufacturing process.

Future research will systematically explore advanced 3D printing strategies and novel material combinations to further improve the mechanical and environmental performance of composite structures. Particular attention will be given to addressing current limitations, such as sample variability and sensitivity to process parameters, that are inherent to additive manufacturing.

Author Contributions: Conceptualization, V.B.; methodology, V.B. and M.B.; validation, V.B., T.H. and K.K.; investigation, V.B., I.B. and M.J.; resources, M.B.; data curation, V.B., I.B., M.B. and M.J.; writing—original draft preparation, V.B.; writing—review and editing, V.B., M.B., R.Č. and Z.P.; visualization, V.B. and M.B.; supervision, M.B. and R.Č.; project administration, M.B. and Z.P.; funding acquisition, Z.P. All authors have read and agreed to the published version of the manuscript.

Funding: This research was supported by the Technological Agency of Czech Republic, project No. FW03010422, and the Grant Agency of the Czech Technical University in Prague, project No. SGS23/149/OHK1/3T/11.

Data Availability Statement: All results are published in the article.

Conflicts of Interest: The authors declare no conflicts of interest.

References

1. Al-Oqla, F.M.; Hayajneh, M.T.; Nawafleh, N. Advanced Synthetic and Biobased Composite Materials in Sustainable Applications: A Comprehensive Review. *Emerg. Mater.* **2023**, *6*, 809–826. [CrossRef]
2. JEC Observer. JEC Observer: Overview of the Global Composites Market 2022–2027. 2023. Available online: https://www.jeccomposites.com/wp-content/uploads/2023/06/v2_14985_DP-UK_JEC-Observer-ECO.pdf (accessed on 1 January 2025).
3. Composites Market: Global Industry Analysis and Forecast (2025–2032). 2025. Available online: https://www.maximizemarketresearch.com/market-report/global-composites-market/34243/ (accessed on 2 February 2025).

4. Grand View Research, Inc. Composites Market Analysis and Segment Forecasts to 2030. 2023. Available online: https://www.grandviewresearch.com/industry-analysis/composites-market (accessed on 12 December 2024).
5. Bullen, G.N.; Grant, C.; Hiken, A.; Day, D.; Champa, D. *Economics of Composites*; SAE International: Warrendale, PA, USA, 2015.
6. Estin, Co. *Overview of the Global Composites Market 2019–2024*; JEC Group: Paris, France, 2020.
7. Lucintel Bio-Composites Market Report: Trends, Forecast and Competitive Analysis. Report and Market. 2020. Available online: https://www.lucintel.com/biocomposite-market.aspx (accessed on 2 January 2025).
8. Brejcha, V.; Kobetičová, K.; Pommer, V.; Koňáková, D.; Böhm, M. Analysis of Porosity and Abrasion Resistance of Composite Material Based on Flax Fiber and Bio-Epoxy Resin with Corundum Additive. In Proceedings of the International Conference of Computational Methods in Sciences and Engineering ICCMSE 2022, Virtual, 26–29 October 2022; AIP Publishing: New York, NY, USA, 2024; Volume 3030, p. 070004.
9. Shirinbayan, M.; Abbasnezhad, N.; Nikooharf, M.H.; Benfriha, K.; Kallel, A.; Jendli, Z.; Fitoussi, J. Manufacturing Process Effect on the Mechanical Properties of Glass Fiber/Polypropylene Composite Under High Strain Rate Loading: Woven (W-GF-PP) and Compressed GF50-PP. *Appl. Compos. Mater.* **2023**, *30*, 1717–1736. [CrossRef]
10. Sathishkumar, T.P.; Satheeshkumar, S.; Naveen, J. Glass Fiber-Reinforced Polymer Composites—A Review. *J. Reinf. Plast. Compos.* **2014**, *33*, 1258–1275. [CrossRef]
11. Zu, Q.; Solvang, M.; Li, H. Commercial Glass Fibers. In *Fiberglass Science and Technology: Chemistry, Characterization, Processing, Modeling, Application, and Sustainability*; Li, H., Ed.; Springer International Publishing: Cham, Switzerland, 2021; pp. 1–87, ISBN 978-3-030-72200-5.
12. Rajak, D.K.; Wagh, P.H.; Linul, E. Manufacturing Technologies of Carbon/Glass Fiber-Reinforced Polymer Composites and Their Properties: A Review. *Polymers* **2021**, *13*, 3721. [CrossRef]
13. Goudenhooft, C.; Siniscalco, D.; Arnould, O.; Bourmaud, A.; Sire, O.; Gorshkova, T.; Baley, C. Investigation of the Mechanical Properties of Flax Cell Walls during Plant Development: The Relation between Performance and Cell Wall Structure. *Fibers* **2018**, *6*, 6. [CrossRef]
14. Rahman, M.M.; Maniruzzaman, M.; Yeasmin, M.S. A State-of-the-Art Review Focusing on the Significant Techniques for Naturally Available Fibers as Reinforcement in Sustainable Bio-Composites: Extraction, Processing, Purification, Modification, as Well as Characterization Study. *Results Eng.* **2023**, *20*, 101511. [CrossRef]
15. Böhm, M.; Brejcha, V.; Jerman, M.; Cerný, R. Bending Characteristics of Fiber-Reinforced Composite with Plywood Balsa Core. In Proceedings of the AIP Conference Proceedings, Rhodes, Greece, 1–5 May 2019; American Institute of Physics Inc.: Melville, NY, USA, 2019; Volume 2186.
16. Scelsi, L.; Hodzic, A.; Soutis, C.; Hayes, S.A.; Rajendran, S.; AlMa'adeed, M.A.; Kahraman, R. A Review on Composite Materials Based on Recycled Thermoplastics and Glass Fibres. *Plast. Rubber Compos.* **2011**, *40*, 1–10. [CrossRef]
17. Tiimob, B.J.; Rangari, V.K.; Jeelani, S. Effect of Reinforcement of Sustainable β-$CaSiO_3$ Nanoparticles in Bio-Based Epoxy Resin System. *J. Appl. Polym. Sci.* **2014**, *131*, 40867. [CrossRef]
18. Nodehi, M. Epoxy, Polyester and Vinyl Ester Based Polymer Concrete: A Review. *Innov. Infrastruct. Solut.* **2021**, *7*, 64. [CrossRef]
19. Krzywiński, K.; Sadowski, Ł.; Stefaniuk, D.; Obrosov, A.; Weiß, S. Engineering and Manufacturing Technology of Green Epoxy Resin Coatings Modified with Recycled Fine Aggregates. *Int. J. Precis. Eng. Manuf. Green Technol.* **2022**, *9*, 253–271. [CrossRef]
20. Kandelbauer, A.; Tondi, G.; Goodman, S.H. *Handbook of Thermoset Plastics: 6 Unsaturated Polyesters and Vinyl Esters Unsaturated Polyesters*; Elsevier: Amsterdam, The Netherlands, 2013.
21. Ramon, E.; Sguazzo, C.; Moreira, P.M.G.P. A Review of Recent Research on Bio-Based Epoxy Systems for Engineering Applications and Potentialities in the Aviation Sector. *Aerospace* **2018**, *5*, 110. [CrossRef]
22. Partanen, A.; Carus, M. Biocomposites, Find the Real Alternative to Plastic—An Examination of Biocomposites in the Market. *Reinf. Plast.* **2019**, *63*, 317–321. [CrossRef]
23. Capretti, M.; Giammaria, V.; Santulli, C.; Boria, S.; Del Bianco, G. Use of Bio-Epoxies and Their Effect on the Performance of Polymer Composites: A Critical Review. *Polymers* **2023**, *15*, 4733. [CrossRef]
24. Stanzione, J.; La Scala, J. Sustainable Polymers and Polymer Science: Dedicated to the Life and Work of Richard P. Wool. *J. Appl. Polym. Sci.* **2016**, *133*, 44212. [CrossRef]
25. Zhang, Y.; Liu, X.; Wan, M.; Zhu, Y.; Zhang, K. Recent Development of Functional Bio-Based Epoxy Resins. *Molecules* **2024**, *29*, 4428. [CrossRef]
26. Sangregorio, A.; Guigo, N.; van der Waal, J.C.; Sbirrazzuoli, N. All 'Green' Composites Comprising Flax Fibres and Humins' Resins. *Compos. Sci. Technol.* **2019**, *171*, 70–77. [CrossRef]
27. Brouwer, W.D. Natural Fibre Composites: Where Can Flax Compete with Glass? *Sampe J.* **2000**, *36*, 18–23.
28. Huda, M.S.; Drzal, L.T.; Ray, D.; Mohanty, A.K.; Mishra, M. Natural-Fiber Composites in the Automotive Sector. In *Properties and Performance of Natural-Fibre Composites*; Elsevier: Amsterdam, The Netherlands, 2008; pp. 221–268.
29. Yan, L.; Chouw, N.; Jayaraman, K. Flax Fibre and Its Composites—A Review. *Compos. B Eng.* **2014**, *56*, 296–317. [CrossRef]

30. Satyanarayana, K.G.; Guimarães, J.L.; Wypych, F. Studies on Lignocellulosic Fibers of Brazil. Part I: Source, Production, Morphology, Properties and Applications. *Compos. Part. A Appl. Sci. Manuf.* **2007**, *38*, 1694–1709. [CrossRef]
31. Shehab, E.; Meiirbekov, A.; Amantayeva, A.; Tokbolat, S. Cost Modelling for Recycling Fiber-Reinforced Composites: State-of-the-Art and Future Research. *Polymers* **2023**, *15*, 150. [CrossRef]
32. Parodo, G.; Sorrentino, L.; Turchetta, S.; Moffa, G. Manufacturing of Sustainable Composite Materials: The Challenge of Flax Fiber and Polypropylene. *Materials* **2024**, *17*, 4768. [CrossRef]
33. Khanal, A.; Shah, A. Techno-Economic Analysis of Hemp Production, Logistics and Processing in the U.S. *Biomass* **2024**, *4*, 164–179. [CrossRef]
34. Dittenber, D.B.; GangaRao, H.V.S. Critical Review of Recent Publications on Use of Natural Composites in Infrastructure. *Compos. Part. A Appl. Sci. Manuf.* **2012**, *43*, 1419–1429. [CrossRef]
35. Genc, G.; El Hafidi, A.; Birame Gning, P. 783. Comparison of the Mechanical Properties of Flax and Glass Fiber Composite Materials. *J. Vibroeng.* **2012**, *14*, 572–581.
36. Ladaci, N.; Saadia, A.; Belaadi, A.; Boumaaza, M.; Chai, B.X.; Abdullah, M.M.S.; Al-Khawlani, A.; Ghernaout, D. ANN and RSM Prediction of Water Uptake of Recycled HDPE Biocomposite Reinforced with Treated Palm Waste W. Filifera. *J. Nat. Fibers* **2024**, *21*, 2356697. [CrossRef]
37. Ramful, R. Mechanical Performance and Durability Attributes of Biodegradable Natural Fibre-Reinforced Composites—A Review. *J. Mater. Sci. Mater. Eng.* **2024**, *19*, 50. [CrossRef]
38. Alzate Acevedo, S.; Díaz Carrillo, Á.J.; Flórez-López, E.; Grande-Tovar, C.D. Recovery of Banana Waste-Loss from Production and Processing: A Contribution to a Circular Economy. *Molecules* **2021**, *26*, 5282. [CrossRef]
39. Kozlowski, R.M. *Handbook of Natural Fibres: Volume 1: Types, Properties and Factors Affecting Breeding and Cultivation*; Elsevier Science & Technology: Chantilly, UK, 2012; ISBN 9780857095503.
40. Nasri, K.; Loranger, É.; Toubal, L. Effect of Cellulose and Lignin Content on the Mechanical Properties and Drop-Weight Impact Damage of Injection-Molded Polypropylene-Flax and -Pine Fiber Composites. *J. Compos. Mater.* **2023**, *57*, 3347–3364. [CrossRef]
41. Yang, J.; Ching, Y.C.; Chuah, C.H. Applications of Lignocellulosic Fibers and Lignin in Bioplastics: A Review. *Polymers* **2019**, *11*, 751. [CrossRef]
42. Komuraiah, A.; Kumar, N.; Prasad, B. Chemical Composition of Natural Fibers and Its Influence on Their Mechanical Properties. *Mech. Compos. Mater.* **2014**, *50*, 359–376. [CrossRef]
43. Kobetičová, K.; Nábělková, J.; Brejcha, V.; Böhm, M.; Jerman, M.; Brich, J.; Černý, R. Ecotoxicity of Caffeine as a Bio-Protective Component of Flax-Fiber-Reinforced Epoxy-Composite Building Material. *Polymers* **2023**, *15*, 3901. [CrossRef] [PubMed]
44. Wang, X.; Petrů, M. Effect of Hygrothermal Aging and Surface Treatment on the Dynamic Mechanical Behavior of Flax Fiber Reinforced Composites. *Materials* **2019**, *12*, 2376. [CrossRef] [PubMed]
45. Guduri, B.R.; Khoathane, C.; Anandjiwala, R.D.; De Vries, A.; Sadiku, E.R.; Van Wyk, L. Effect of Water Absorption on Mechanical Properties of Flax Fibre Reinforced Composites. *Adv. Sci. Technol. Res. J.* **2015**, *9*, 1–6.
46. Kim, Y.K.; Chalivendra, V. Natural Fibre Composites (NFCs) for Construction and Automotive Industries. In *Handbook of Natural Fibres*; Elsevier: Amsterdam, The Netherlands, 2020; pp. 469–498.
47. Li, X.; Tabil, L.G.; Panigrahi, S. Chemical Treatments of Natural Fiber for Use in Natural Fiber-Reinforced Composites: A Review. *J. Polym. Environ.* **2007**, *15*, 25–33. [CrossRef]
48. Ventura, H.; Claramunt, J.; Navarro, A.; Rodriguez-Perez, M.A.; Ardanuy, M. Effects of Wet/Dry-Cycling and Plasma Treatments on the Properties of Flax Nonwovens Intended for Composite Reinforcing. *Materials* **2016**, *9*, 93. [CrossRef]
49. Rachtanapun, P.; Sawangrat, C.; Kanthiya, T.; Kaewpai, K.; Thipchai, P.; Tanadchangsaeng, N.; Worajittiphon, P.; Suhr, J.; Wattanachai, P.; Jantanasakulwong, K. Comparison of Effects of Plasma Surface Modifications of Bamboo and Hemp Fibers on Mechanical Properties of Fiber-Reinforced Epoxy Composites. *Polymers* **2024**, *16*, 3394. [CrossRef]
50. Sassi, F.Z.; Zouari, R.; Baffoun, A.; Sonnier, R.; Longuet, C.; Khemir, H.; Msahli, S. Plasma Jet Technology to Improve the Hydrophobicity of Flax Fabrics. In Proceedings of 10th International Conference of Applied Research on Textile and Materials, Monastir, Tunisia, 9–11 November 2023; Babay, A., Cheriaa, R., Zouari, R., Eds.; Springer: Cham, Switzerland, 2024; pp. 113–117.
51. Bayart, M.; Gauvin, F.; Foruzanmehr, M.R.; Elkoun, S.; Robert, M. Mechanical and Moisture Absorption Characterization of PLA Composites Reinforced with Nano-Coated Flax Fibers. *Fibers Polym.* **2017**, *18*, 1288–1295. [CrossRef]
52. Gieparda, W.; Rojewski, S.; Rózanska, W. Effectiveness of Silanization and Plasma Treatment in the Improvement of Selected Flax Fibers' Properties. *Materials* **2021**, *14*, 3564. [CrossRef]
53. Koohestani, B.; Darban, A.K.; Mokhtari, P.; Yilmaz, E.; Darezereshki, E. Comparison of Different Natural Fiber Treatments: A Literature Review. *Int. J. Environ. Sci. Technol.* **2019**, *16*, 629–642. [CrossRef]
54. Thyavihalli Girijappa, Y.G.; Mavinkere Rangappa, S.; Parameswaranpillai, J.; Siengchin, S. Natural Fibers as Sustainable and Renewable Resource for Development of Eco-Friendly Composites: A Comprehensive Review. *Front. Mater.* **2019**, *6*, 226. [CrossRef]

55. Shahria, S. Fabrication and Property Evaluation of Hemp-Flax Fiber Reinforced Hybrid Composite. *Chem. Mater. Eng.* **2019**, *7*, 17–23. [CrossRef]
56. Stelea, L.; Filip, I.; Lisa, G.; Ichim, M.; Drobotă, M.; Sava, C.; Mureșan, A. Characterisation of Hemp Fibres Reinforced Composites Using Thermoplastic Polymers as Matrices. *Polymers* **2022**, *14*, 481. [CrossRef] [PubMed]
57. Stochioiu, C.; Ciolcă, M.; Deca, A.L. Mechanical Characterization of Flax and Hemp Fibers Cultivated in Romania. *Materials* **2024**, *17*, 4871. [CrossRef]
58. Liu, H.; Yu, Y.; Liu, Y.; Zhang, M.; Li, L.; Ma, L.; Sun, Y.; Wang, W. A Review on Basalt Fiber Composites and Their Applications in Clean Energy Sector and Power Grids. *Polymers* **2022**, *14*, 2376. [CrossRef]
59. Deng, X.; Hoo, M.S.; Cheah, Y.W.; Tran, L.Q.N. Processing and Mechanical Properties of Basalt Fibre-Reinforced Thermoplastic Composites. *Polymers* **2022**, *14*, 1220. [CrossRef]
60. Holmes, M. Biocomposites Take Natural Step Forward: Applications for Biocomposites and the Use of Natural Fiber Reinforcements Are Increasing. Reinforced Plastics Looks at a Number of Examples. *Reinf. Plast.* **2019**, *63*, 194–201. [CrossRef]
61. Pawlik, M.; Gunputh, U.; Odiyi, D.; Odofin, S.; Le, H.; Wood, P.; Maligno, A.; Lu, Y. Mechanical Properties of Eco-Friendly, Lightweight Flax and Hybrid Basalt/Flax Foam Core Sandwich Panels. *Materials* **2024**, *17*, 3842. [CrossRef]
62. Alphonse, M.; Bupesh Raja, V.K.; Gopala Krishna, V.; Kiran, R.S.U.; Subbaiah, B.V.; Chandra, L.V.R. Mechanical Behavior of Sandwich Structures with Varying Core Material—A Review. *Mater. Today Proc.* **2021**, *44*, 3751–3759. [CrossRef]
63. Yan, J.; Wang, G.; Li, Q.; Zhang, L.; Yan, J.D.; Chen, C.; Fang, Z. A Comparative Study on Damage Mechanism of Sandwich Structures with Different Core Materials under Lightning Strikes. *Energies* **2017**, *10*, 1594. [CrossRef]
64. Imielińska, K.; Guillaumat, L.; Wojtyra, R.; Castaings, M. Effects of Manufacturing and Face/Core Bonding on Impact Damage in Glass/Polyester-PVC Foam Core Sandwich Panels. *Compos. B Eng.* **2008**, *39*, 1034–1041. [CrossRef]
65. Kausar, A.; Ahmad, I.; Rakha, S.A.; Eisa, M.H.; Diallo, A. State-of-the-Art of Sandwich Composite Structures: Manufacturing-to-High Performance Applications. *J. Compos. Sci.* **2023**, *7*, 102. [CrossRef]
66. Jang, J.-W.; Jeong, S.; Oh, D.; Cho, J.-H.; Noh, J. Test and Evaluation Procedure of Foam Core Materials for Composite Ships. *J. Korean Soc. Mar. Environ. Saf.* **2020**, *26*, 286–296. [CrossRef]
67. Pertiwi, Y.A.B.; Ishiguri, F.; Aiso, H.; Ohshima, J.; Yokota, S. Wood Properties of 7-Year-Old Balsa (*Ochroma pyramidale*) Planted in East Java. *Int. Wood Prod. J.* **2017**, *8*, 227–232. [CrossRef]
68. Easterling, K.E.; Harrysson, R.; Gibson, L.J.; Ashby, M.F. On the Mechanics of Balsa and Other Woods. *Proc. R. Soc. Lond. Ser. A Math. Phys. Sci.* **1982**, *383*, 31–41.
69. Kotlarewski, N.J.; Belleville, B.; Gusamo, B.K.; Ozarska, B. Mechanical Properties of Papua New Guinea Balsa Wood. *Eur. J. Wood Wood Prod.* **2016**, *74*, 83–89. [CrossRef]
70. Jagadeesh, P.; Puttegowda, M.; Rangappa, S.M.; Alexey, K.; Gorbatyuk, S.; Khan, A.; Doddamani, M.; Siengchin, S. A Comprehensive Review on 3D Printing Advancements in Polymer Composites: Technologies, Materials, and Applications. *Int. J. Adv. Manuf. Technol.* **2022**, *121*, 127–169. [CrossRef]
71. Delgado Camacho, D.; Clayton, P.; O'Brien, W.J.; Seepersad, C.; Juenger, M.; Ferron, R.; Salamone, S. Applications of Additive Manufacturing in the Construction Industry—A Forward-Looking Review. *Autom. Constr.* **2018**, *89*, 110–119. [CrossRef]
72. Wimpenny, D.I.; Pandey, P.M.; Jyothish Kumar, L. *Advances in 3D Printing & Additive Manufacturing Technologies*; Springer: Singapore, 2016; ISBN 9789811008122.
73. Ansari, A.I.; Sheikh, N.A. A Review on Different Approaches for Foam Fabrication. *J. Inst. Eng. Ser. C* **2023**, *104*, 1219–1245. [CrossRef]
74. Zheng, X.; Williams, C.; Spadaccini, C.M.; Shea, K. Perspectives on Multi-Material Additive Manufacturing. *J. Mater. Res.* **2021**, *36*, 3549–3557. [CrossRef]
75. Bryll, K.; Piesowicz, E.; Szymański, P.; Slaczka, W.; Pijanowski, M. Polymer Composite Manufacturing by FDM 3D Printing Technology. *MATEC Web Conf.* **2018**, *237*, 02006. [CrossRef]
76. Lumpe, T.S.; Shea, K. Computational Design of 3D-Printed Active Lattice Structures for Reversible Shape Morphing. *J. Mater. Res.* **2021**, *36*, 3642–3655. [CrossRef]
77. Marabello, G.; Borsellino, C.; Di Bella, G. Carbon Fiber 3D Printing: Technologies and Performance—A Brief Review. *Materials* **2023**, *16*, 7311. [CrossRef] [PubMed]
78. Ghosh, B.; Karmakar, S. 3D Printing Technology and Future of Construction: A Review. In Proceedings of the IOP Conference Series: Earth and Environmental Science, Jaipur, India, 11–12 August 2023; Institute of Physics: Melville, NY, USA, 2024; Volume 1326.
79. Ning, X.; Liu, T.; Wu, C.; Wang, C. 3D Printing in Construction: Current Status, Implementation Hindrances, and Development Agenda. *Adv. Civ. Eng.* **2021**, *2021*, 6665333. [CrossRef]
80. Jayakrishna, M.; Vijay, M.; Khan, B. An Overview of Extensive Analysis of 3D Printing Applications in the Manufacturing Sector. *J. Eng.* **2023**, *2023*, 7465737. [CrossRef]

81. Nodehi, M.; Ozbakkaloglu, T.; Gholampour, A. Effect of Supplementary Cementitious Materials on Properties of 3D Printed Conventional and Alkali-Activated Concrete: A Review. *Autom. Constr.* **2022**, *138*, 104215. [CrossRef]
82. Rehman, A.U.; Kim, J.H. 3d Concrete Printing: A Systematic Review of Rheology, Mix Designs, Mechanical, Microstructural, and Durability Characteristics. *Materials* **2021**, *14*, 3800. [CrossRef]
83. Momeni, K.; Vatin, N.I.; Hematibahar, M.; Gebre, T.H. Differences between 3D Printed Concrete and 3D Printing Reinforced Concrete Technologies: A Review. *Front. Built Environ.* **2024**, *10*, 1450628. [CrossRef]
84. Sun, H.Q.; Zeng, J.J.; Hong, G.Y.; Zhuge, Y.; Liu, Y.; Zhang, Y. 3D-Printed Functionally Graded Concrete Plates: Concept and Bending Behavior. *Eng. Struct.* **2025**, *327*, 119551. [CrossRef]
85. Qi, C.; Jiang, F.; Yang, S. Advanced Honeycomb Designs for Improving Mechanical Properties: A Review. *Compos. B Eng.* **2021**, *227*, 109393. [CrossRef]
86. Blok, L.G.; Longana, M.L.; Yu, H.; Woods, B.K.S. An Investigation into 3D Printing of Fibre Reinforced Thermoplastic Composites. *Addit. Manuf.* **2018**, *22*, 176–186. [CrossRef]
87. Sugiyama, K.; Matsuzaki, R.; Ueda, M.; Todoroki, A.; Hirano, Y. 3D Printing of Composite Sandwich Structures Using Continuous Carbon Fiber and Fiber Tension. *Compos. Part. A Appl. Sci. Manuf.* **2018**, *113*, 114–121. [CrossRef]
88. Deng, K.; Khan, M.H.U.; Park, S.; Sung, D.H.; Fu, K. Additive Manufacturing of Continuous Carbon Fiber/Epoxy Composites with Structured Core-Shell Towpreg: Methods, Characterization, and Mechanics. *Compos. B Eng.* **2025**, *291*, 112001. [CrossRef]
89. Andrzejewski, J.; Gronikowski, M.; Aniśko, J. A Novel Manufacturing Concept of LCP Fiber-Reinforced GPET-Based Sandwich Structures with an FDM 3D-Printed Core. *Materials* **2022**, *15*, 5405. [CrossRef]
90. Lu, C.; Qi, M.; Islam, S.; Chen, P.; Gao, S.; Xu, Y.; Yang, X. Mechanical Performance of 3D-Printing Plastic Honeycomb Sandwich Structure. *Int. J. Precis. Eng. Manuf. Green Technol.* **2018**, *5*, 47–54. [CrossRef]
91. 3D LabPrint Technical Data Sheet and Specification of PolyLight 1.0. Available online: https://3dlabprint.com/faq/prusaslicer/ (accessed on 18 October 2024).
92. Nofar, M.; Utz, J.; Geis, N.; Altstädt, V.; Ruckdäschel, H. Foam 3D Printing of Thermoplastics: A Symbiosis of Additive Manufacturing and Foaming Technology. *Adv. Sci.* **2022**, *9*, 2105701. [CrossRef]
93. Loh, G.H.; Pei, E.; Gonzalez-Gutierrez, J.; Monzón, M. An Overview of Material Extrusion Troubleshooting. *Appl. Sci.* **2020**, *10*, 4776. [CrossRef]
94. Sun, B.; Wu, L. Research Progress of 3D Printing Combined with Thermoplastic Foaming. *Front. Mater.* **2022**, *9*, 1083931. [CrossRef]
95. Ashraf, W.; Ishak, M.R.; Zuhri, M.Y.M.; Yidris, N.; Ya'acob, A.M. Effect on Mechanical Properties by Partial Replacement of the Glass with Alkali-Treated Flax Fiber in Composite Facesheet of Sandwich Structure. *J. Mater. Res. Technol.* **2021**, *13*, 89–98. [CrossRef]
96. Sadeghian, P.; Hristozov, D.; Wroblewski, L. Experimental and Analytical Behavior of Sandwich Composite Beams: Comparison of Natural and Synthetic Materials. *J. Sandw. Struct. Mater.* **2018**, *20*, 287–307. [CrossRef]
97. Shaker, K.; Nawab, Y.; Jabbar, M. Bio-Composites: Eco-Friendly Substitute of Glass Fiber Composites. In *Handbook of Nanomaterials and Nanocomposites for Energy and Environmental Applications*; Kharissova, O.V., Martínez, L.M.T., Kharisov, B.I., Eds.; Springer International Publishing: Cham, Switzerland, 2020; pp. 1–25, ISBN 978-3-030-11155-7.
98. Patel, R.V.; Yadav, A.; Winczek, J. Physical, Mechanical, and Thermal Properties of Natural Fiber-Reinforced Epoxy Composites for Construction and Automotive Applications. *Appl. Sci.* **2023**, *13*, 5126. [CrossRef]
99. Khan, F.M.; Shah, A.H.; Wang, S.; Mehmood, S.; Wang, J.; Liu, W.; Xu, X. A Comprehensive Review on Epoxy Biocomposites Based on Natural Fibers and Bio-Fillers: Challenges, Recent Developments and Applications. *Adv. Fiber Mater.* **2022**, *4*, 683–704. [CrossRef]
100. Böhm, M.; Brejcha, V.; Kobetičová, K.; Procházka, J.; Krejsová, J.; Koňáková, D.; Černý, R.; Polášek, M.; Heneberg, P.; Němcová, D. *Composite Shell Element, Czech Utility Model 37723*; Industrial Property Office of the Czech Republic: Prague, Czech Republic, 2024.
101. Cao, D.; Bouzolin, D.; Lu, H.; Griffith, D.T. Bending and Shear Improvements in 3D-Printed Core Sandwich Composites through Modification of Resin Uptake in the Skin/Core Interphase Region. *Compos. B Eng.* **2023**, *264*, 110912. [CrossRef]
102. Zeng, J.J.; Yan, Z.T.; Jiang, Y.Y.; Li, P.L. 3D Printing of FRP Grid and Bar Reinforcement for Reinforced Concrete Plates: Development and Effectiveness. *Compos. Struct.* **2024**, *335*, 117946. [CrossRef]
103. Konsta-Gdoutos, M.S.; Gdoutos, E.E. The Effect of Load and Geometry on the Failure Modes of Sandwich Beams. *Appl. Compos. Mater.* **2005**, *12*, 165–176. [CrossRef]
104. Da Silva, A.; Kyriakides, S. Compressive Response and Failure of Balsa Wood. *Int. J. Solids Struct.* **2007**, *44*, 8685–8717. [CrossRef]
105. Al-Hamdan, A.; Ajlouni, M.; Alhusein, M.; Rudd, C.; Long, A. Behaviour of Core Materials during Resin Transfer Moulding of Sandwich Structures. *Mater. Sci. Technol.* **2000**, *16*, 929–934. [CrossRef]

106. Schlimper, R.; Müller, M.; Willner, F.; Schäuble, R. Resin Absorption and Deformation Behaviour of Foam Core Materials for High Performance Sandwich Panels. In Proceedings of the 14th European Conference on Composite Materials, Budapest, Hungary, 7–10 June 2010.
107. Cullen, R.K.; Grove, S.M.; Summerscales, J. Resin infusion of sandwich structures—Core/skin interactions and void formation. In Proceedings of the ICCM International Conferences on Composite Materials, Edinburgh, Scotland, 27–31 September 2009.